Available online at www.sciencedirect.com

ScienceDirect

Journal of Nuclear Materials 358 (2006) 57–68

journal of nuclear materials

www.elsevier.com/locate/jnucmat

The ion exchange phase in corrosion of nuclear waste glasses

Michael I. Ojovan [a,*], Alexey Pankov [a], William E. Lee [b]

[a] *Immobilisation Science Laboratory, Department of Engineering Materials, University of Sheffield, Sir Robert Hadfield Building, Mappin Street, Sheffield S1 3JD, United Kingdom*

[b] *Department of Materials, Imperial College London, South Kensington Campus, London SW7 2AZ, United Kingdom*

Received 10 April 2006; accepted 30 June 2006

Abstract

The diffusion-controlled ion exchange phase in the corrosion of nuclear waste borosilicate glasses has been examined using the Doremus' model accounting for interdiffusion and exchange of the cations in the glass with protons from the water. Ion exchange is the principal radionuclide release mechanism for conditions when glass network hydrolysis is suppressed, such as in silica-saturated solutions when ion exchange may persist over geological time scales. In dilute aqueous solutions ion exchange controls the initial cation release and can dominate for tens and many hundreds of years if temperatures are low at low and neutral pH. Ion exchange rates are shown to have inverse square root time dependences, an Arrhenius-controlled temperature relationship and a $10^{-0.5\text{pH}}$ dependence with the pH of the contacting water. Due to radioactive decay the radionuclide releases from nuclear waste glasses are limited to certain upper values, which can be calculated based on available experimental data.

PACS: 81.05.Kf; 82.65.+r; 82.20.Db; 82.30.Fi

---

1. Introduction

Studies of archaeological artefacts show that the principal processes in the natural corrosion of silicates are diffusion-controlled ion exchange reactions leading to selective leaching of alkalis and protons entering the silicate structure to produce a hydrated alkali-deficient layer and congruent dissolution with destruction of the silicate network and subsequent precipitation of hydrous silica-gel layers as secondary alteration products [1,2]. At ambient temperatures the ion exchange reactions persist for extended periods of time and govern alteration processes for thousands [1] and tens of thousands [2] of years. The role of ion exchange in the corrosion behaviour of nuclear waste glasses is also considered to be important [3–5]. Insight into long term behaviour of nuclear waste glasses is an important issue related to our ability to assess the reliability of nuclear waste immobilisation in an envisaged repository environment [3]. Corrosion of nuclear waste glasses is a complex process which depends on many parameters such as glass composition

---

[*] Corresponding author. Tel.: +44 114 2226033; fax: +44 114 2225943.

E-mail address: m.ojovan@sheffield.ac.uk (M.I. Ojovan).

0022-3115/$ - see front matter © 2006 Elsevier B.V. All rights reserved.
doi:10.1016/j.jnucmat.2006.06.016

and radionuclide content, time, temperature, groundwater chemical composition and pH. The best approach to quantifying its functional dependence is to determine the basic parameters governing the corrosion so that various scenarios can be modelled in the performance assessment of a future repository. Corrosion of silicate glasses including nuclear waste-containing borosilicate glasses involves two major processes – diffusion-controlled ion exchange and glass network hydrolysis [6,7]. In this paper we consider the diffusion-controlled ion exchange phase of glass corrosion. Indeed ion exchange plays an important role in the behaviour of silicate glasses including nuclear waste glasses in aqueous solutions being the principal release mechanism in conditions when the glass network hydrolysis is suppressed, such as in silica-saturated solutions when it may persist over geological time scales. In dilute near neutral solutions ion exchange controls the initial cation releases whereas hydrolysis of the glass network is responsible for the later stages of corrosion. The transition times from ion exchange to hydrolysis are relatively short only at high temperatures spanning from hours to several days. In contrast at low temperatures the ion exchange processes can dominate over hydrolysis for tens and many hundreds of years before hydrolysis will turn out to be significant in the total inventory of released cations [4,5,8].

Consider corrosion behaviour of vitrified nuclear wastes in an envisaged repository environment. The release of radioactive species, which in nuclear waste glasses are solely represented by radioactive cations, can be caused by corrosion of the glass in contact with groundwater. However, the potential contact of water with glass is deferred in actual disposal systems to times after the waste container has been breached. For vitrified high-level waste (HLW) containers, which are made of stainless steel, these times may be of the order of many hundreds or even thousands of years [9]. High temperatures and radiation dose rates are likely only for the first few hundred years after HLW vitrification so that container temperatures will be close to those of the ambient rock by the expected time of contact with groundwater. Moreover the role of $\beta\gamma$-radiolysis will also become negligible because of low radiation dose rates. For example, the dose rate at the contact of an industrial R7T7 nuclear waste glass canister is 872 Gy/h after 30 years from vitrification, but drops to just ~0.07 Gy/h after 500 years [10]. Nonetheless the alteration of glass caused by irradiation may become important at these times due to high absorbed doses of radiation and may affect the rates of ion exchange [11]. Vitrification continues to be used for immobilisation of HLW [12–14] and is also currently deployed for low and intermediate waste (LILW) as a viable alternative to cementation [14–18]. Vitrified LILW is almost invariably at the ambient temperature of a repository environment. In addition this type of waste is expected to be disposed of in near-surface repositories which are often characterised by near-neutral groundwaters and relatively low host rock temperatures [19]. Hence the temperatures of nuclear waste glasses at the times of expected contact with groundwater are likely to be close to those of the surrounding repository environment. As these temperatures are below several tens of degrees centigrade the corrosion of glasses will occur via ion exchange for very long times even in contact with non-silica saturated groundwater. This paper focuses on this case although the ion exchange controls corrosion of glasses at geological timescales when the contacting groundwater is silica-saturated and the hydrolytic dissolution of the glass network is impeded.

The Doremus' theory of interdiffusion has been used to model the diffusion-controlled ion exchange corrosion of glass in this work [20] in which the Agaard–Helgeson transition state theory is used to assess the transition times to hydrolysis-controlled corrosion [21]. It has been revealed that due to radioactive decay the radionuclide releases from nuclear waste glasses cannot exceed certain upper values, which can be calculated based on available experimental data.

2. Diffusion-controlled ion exchange and hydrolysis

Two basic mechanisms control the water corrosion of silicate glasses and hence the release of cationic species from glasses: diffusion-controlled ion exchange and hydrolysis [6,7,22,23]. The ion exchange reaction of glass with water can be written as

$$(\equiv\text{Si–O-Cation})_{\text{glass}} + H_2O \leftrightarrow (\equiv\text{Si–O–H})_{\text{glass}} + \text{Cation-OH}. \quad (1)$$

This reaction is controlled by the counter diffusion of protons (probably as H_3O^+) from the water which replace cations in the glass structure e.g. cations bonded to non-bridging oxygens (NBO)

[3]. The rate of release of the ith cation into water via diffusion-controlled ion exchange rx_i (g/cm^2 d) is given by the magnitude of the flux of species through the surface of glass i.e. $rx_i = |\vec{J}_{\mathrm{di}}| = J_{\mathrm{di}}$ at the glass–water interface. The diffusion flux of cations is given by Fick's first law

$$\vec{J}_{\mathrm{di}} = -D_i \vec{\nabla} C_i, \tag{2}$$

where C_i is the cation concentration in the glass (g/cm^3) and D_i is the effective diffusion coefficient (cm^2/d). D_i has an Arrhenius-type temperature dependence and can be written as

$$D_i = D_{0i} \exp\left(-\frac{E_{\mathrm{di}}}{RT}\right), \tag{3}$$

where D_{0i} is the pre-exponential term (cm^2/d), T is the absolute temperature (K), R is the molar gas constant and E_{di} is the activation energy of effective diffusion (kJ/mol).

The hydrolysis of silicate glass occurs via

$$\equiv\mathrm{Si{-}O{-}Si}\equiv + \mathrm{H_2O} \leftrightarrow 2(\equiv\mathrm{SiOH}). \tag{4}$$

Hydrolysis results in complete dissolution of the glass network and formation of silicic acid H_4SiO_4. This process leads to a congruent to the glass composition release of glass constituents into the water. The hydrolytic flux of species is given by $\vec{J}_{h_i}(\vec{r}, t) = \rho f_i r_{\mathrm{h}} \vec{n}$ where r_{h} is the stationary hydrolysis (dissolution) rate of the glass, e.g. the steady state rate of motion of the hydrolysis front into the glass. Note that generally r_{h} is not equal to the measured rate of decrease of glass thickness because of de-hydroxylation reactions and silicic acid re-precipitation as hydrated silica gel ($H_2SiO_3 nH_2O$) [7]. The rate of hydrolysis, r_{h} (μm/y), is determined by the transition state theory of silicate mineral dissolution of Agaard and Helgeson [21] and can be expressed as

$$r_{\mathrm{h}} = r_{\mathrm{oc}} \exp\left(-\frac{E_{\mathrm{a}}}{RT}\right), \tag{5}$$

where

$$r_{\mathrm{oc}} = k a_{\mathrm{H^+}}^{-\eta} [1 - (Q/K)^{\sigma}], \tag{6}$$

where k is the intrinsic rate constant, $a_{\mathrm{H+}}$ is the hydrogen ion activity, η is the pH power law coefficient, E_{a} is the activation energy and Q the ion-activity product of the rate controlling reaction, K is the pseudo-equilibrium constant of this reaction and σ is the net reaction order. The affinity term $[1 - (Q/K)^{\sigma}]$ characterises the decrease in solution aggressiveness with respect to the glass as it becomes increasingly concentrated in dissolved elements and as the ion activity product Q of the reactive species approaches the material solubility product K, e.g. $r_{\mathrm{oc}} \to 0$, when $Q \to K$. In dilute aqueous systems when $K \ll Q$ the affinity term is simply equal to unity $[1 - (Q/K)^{\sigma}] = 1$. Note that $\eta = 0.5$ [24] and the higher the pH of the attacking water solution the higher the rate of hydrolysis. Hydrolysis prevails in corrosion of silicate glasses at normal temperatures when pH exceeds 9–10 [6,25,26]. However, the higher the temperature the more important the hydrolysis reactions become and these dominate even at low pH if temperatures are high [6,27]. Hence it is necessary to consider both pH and temperature when identifying the major corrosion mechanisms. A useful tool in understanding is to construct time–temperature diagrams of the corrosion mechanisms [27,28].

Both ion exchange and hydrolysis contribute to aqueous glass corrosion thus the total rate of released species into the water is given by the sum $r_i = r_{xi} + r_{\mathrm{h}}$. Because of rapid dissolution of near surface layers, which are different from the bulk [29,30], there is an additional contribution to this sum termed instantaneous surface dissolution, although this is a short-term transient effect [8,31]. Depending on glass composition and conditions of aqueous corrosion as well as on time the contribution of the two basic mechanisms to the overall corrosion rate, as we will discuss below, can be different.

2.1. Time–temperature diagrams

Corrosion mechanisms of glasses can change with time even at constant and near neutral pH and constant temperature of contacting water. This occurs not because of changes in the contacting water which is considered here to be diluted and with its parameters unchanging either due to its very large volume comparing the glass or due to its flow regime. The ion exchange reaction of glass with water leads to gradual diminution of cation content in the near surface glass layers. Because of this depletion in the glass near surface layers over time the rate of ion-exchange diminishes. In contrast the rate of glass hydrolysis, although small in near-neutral conditions, remains constant. Hence hydrolysis will eventually dominate, once the near-surface glass layers have become depleted in cations [6,8,27,28]. This occurs except under silica saturated conditions when the rate of hydrolysis, r_h (μm/y), is negligibly small.

The time required for silicate glasses to reach the hydrolysis stage in near-neutral solutions depends mainly on glass composition and temperature. Note that we suppose unchanged water parameters so there is no coupling between water chemistry and the corroding glass. More highly polymerised glasses are hydrolytically decomposed more slowly [6]. Thus glasses with higher silica contents require longer times before hydrolysis becomes dominant compared to high sodium content glasses [6,27]. Previous work by the authors has suggested that the corrosion regimes of silicate glasses should be characterised in terms of time–temperature parameters as the higher the temperature the sooner hydrolysis becomes dominant [3,8,27,28]. This occurs because the activation energy for hydrolysis, E_a, is significantly higher than the activation energies of diffusive processes E_{di}. It has been shown that the diffusion-controlled ion exchange stage is dominant up to a time, $\tau(T)$, given by [8,27,28]

$$\tau(T) = \tau_0 \exp\left(\frac{2E_a - E_{di}}{RT}\right), \qquad (7)$$

where τ_0 is a pre-exponential term (days)

$$\tau_0 = \frac{D_{0i}}{r_{oc}^2}. \qquad (8)$$

Note that the time τ_0 diverges with silica concentrations approaching the solubility limit when $Q \to K$ because according to (6) $r_{oc} \to 0$, demonstrating that the only important cation release mechanism remains ion exchange in this case. Moreover the hydrolytic stage of glass corrosion is dominant when time $t \geqslant 16\tau(T)$, whereas within $\tau(T) \leqslant t \leqslant 16\tau(T)$ the glass corrodes with equivalent contributions from both ion exchange and hydrolysis [8,27,28].

We have previously reported on the time–temperature behaviour of Russian K-26 nuclear waste glass [8], whereas here we will characterise the behaviour of UK Magnox-waste glass. A previous study [32] demonstrated that in near-neutral water solutions UK Magnox-waste glass undergoes incongruent ion-exchange over a period of 28 days even at temperatures as high as 60–90 °C. Based on this work we can estimate $\tau(60\ ^\circ\mathrm{C}) \approx 28\mathrm{d}$, $E_a \approx 60\ \mathrm{kJ\ mol^{-1}}$ and $E_{di} \approx 36\ \mathrm{kJ\ mol^{-1}}$ to enable tentative identification of the most likely scenarios for corrosion of UK Magnox-waste glass as a function of temperature and time (Fig. 1).

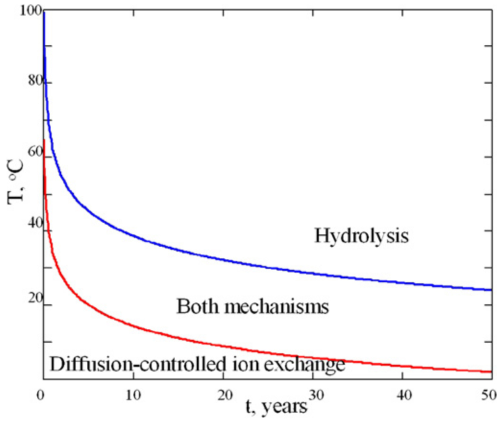

Fig. 1. Corrosion mechanisms for British Magnox-waste glass in deionised water.

Fig. 1 shows that corrosion in deionised water at a constant temperature begins with a fully controlled ion exchange phase. As the corrosion progresses the impact of hydrolysis becomes significant with comparable contributions from both basic mechanisms. Finally, the glass corrosion in deionised water is fully controlled by hydrolysis. The characteristic time which indicates the duration of pure ion exchange phase is given by Eq. (7). Table 1 gives some values of the characteristic times $\tau(T)$ for a number of glasses corroding in non-Si-saturated near neutral water solutions.

2.2. Rates of ion exchange

In Doremus' model the ion exchange involves interdiffusion and exchange of the cations in the glass with a proton (probably as H_3O^+) from the water and results in an interdiffusion flux of cations replaced by the H^+ (or hydronium) ion [20]:

Table 1
Transition times for the intermediate stage of glass dissolution

Glass	T (°C)	τ (T)	References
British Magnox-waste	90	>28 days	[32]
USA SRL131A, SRL202A	25	>240 days	[25]
Russian Bs-10	11	3.2 years	Calculated using data from [27]
Russian K-26	4.5	16.4 years	[8]
Roman IF (Archaeological)	14–15	~1800 years	[1]

Note that an increase of contacting water pH would decrease characteristic transition times.

$\vec{J}_{di}(\vec{r},t) = -D_{iH}\vec{\nabla}C_i$, where the interdiffusion coefficient D_{iH} in an ideal case is given by the Nernst–Planck equation $D_{iH} = D_iD_H/(D_iN_i + D_HN_H)$. D_i and D_H are the diffusion coefficients of the cations in the glass and replacement hydrogen containing ions (whether H^+ or H_3O^+), N_i and N_H are molar fractions of the cations and hydrogen-containing ions respectively, *i.e.* $N_i + N_H = 1$. The effective diffusion coefficient in Eq. (6) within the framework of Doremus' model is $D_i \equiv D_{iH}$. The interdiffusion coefficient depends on the concentrations of both diffusing ions and hence on coordinate (space locus) although experiments indicate that $D_H \ll D_i$. Moreover because $N_HD_H \ll N_iD_i$ the interdiffusion coefficient is approximately given by $D_{iH} \cong D_H/N_i$. Secondary ion mass spectrometry depth profiles of corroded silicate glasses show that at the water-glass interface the concentration of protons significantly exceeds that of monovalent cations such as sodium and potassium [33]. Thus the molar fraction of cation i in the glass at the glass surface can be supposed with a high degree of accuracy as $N_i \approx C_i/C_H$. Hence within Doremus' approach we conclude that the interdiffusion coefficient, D_{iH}, and therefore the effective diffusion coefficient of released species, D_i, is directly proportional to proton concentration, C_H

$$D_{iH} \cong D_HC_H/C_i. \tag{9}$$

This result is in excellent agreement with experimental findings [2], which reveal for water-altered quartz an Arrhenius temperature behaviour and linear dependency with C_H for the effective diffusivity. Note that the concentration of protons at the glass surface is proportional to the concentration of protons (hydronium) in the water $C_H = \kappa C_{Hsol}$, where κ is a constant and $C_{Hsol} = 1(\text{mol/L})10^{-pH}$. Hence the interdiffusion coefficient can be expressed as a function of the pH of the contacting water

$$D_{iH} \cong \alpha_iD_H10^{-pH}, \tag{10}$$

where the dimensionless parameter $\alpha_i = \kappa/C_i(0)$ and concentration of species at the glass surface, $C_i(0)$, is taken in mol/L. The rates of cation release via diffusion-controlled ion exchange are determined from Eq. (2). The cation concentration gradient at the glass–water interface can be found using

$$|\vec{\nabla}C_i| = \frac{\overline{C}_i - C_{isol}}{\pi^{1/2}L_i}, \tag{11}$$

where $\overline{C}_i$ is the average cation concentration in the glass, C_{isol} is the concentration of cations in the water solution (g/cm^3) and L_i is the diffusion length (cm) given by the Einstein relation

$$L_i = (D_it)^{1/2}. \tag{12}$$

As the concentration of cations in water solutions is always supposed to be much smaller than in the glass *i.e.* $C_{isol} \ll \overline{C}_i$, this term can be neglected hence

$$|\vec{\nabla}C_i| \cong \frac{\overline{C}_i}{\pi^{1/2}L_i}. \tag{13}$$

Given that $\overline{C}_i = f_i\rho$, where ρ is the density of the glass (g/cm^3) and f_i is the mass fraction of the ith cation in the glass, combining Eqs. (2), (3) and (13) gives the rate of cation release via ion exchange as

$$rx_i = \rho f_i\left(\frac{D_{0i}}{\pi t}\right)^{1/2}\exp\left(-\frac{E_{di}}{2RT}\right). \tag{14}$$

Ion exchange involves the interdiffusion and exchange of cations in the glass with a proton (probably as H_3O^+) from the water. Because cations in glasses are bound to NBO the activation energy for interdiffusion is the sum of the enthalpy of motion of protons, H_{mH}, and the enthalpy of formation of NBO, H_{fNBO}, [34]

$$E_{di} = H_{mH} + H_{fNBO}. \tag{15}$$

Note that the activation energy of interdiffusion holds the same value for all monovalent cations because proton ingress into the glass is the limiting step [8]. Within the framework of Doremus' model $D_i \equiv D_{iH}$ hence from (10) it follows that the pre-exponential coefficient of the interdiffusion coefficient can also be expressed as a function of the pH of the contacting water $D_{0i} = \alpha_iD^*_{0H}10^{-pH}$, where D^*_{0H} is the pre-exponential coefficient in the diffusion coefficient for protons in the glass $D_H = D^*_{0H}\exp(-E_{dH}/RT)$, and E_{dH} is the activation energy for diffusion of protons in the glass. As a result the rate of release of species via ion-exchange is finally given by

$$rx_i = \rho f_i\left(\frac{\alpha_iD^*_{0H}}{\pi t}\right)^{1/2}10^{-0.5pH}\exp\left(-\frac{E_{di}}{2RT}\right). \tag{16}$$

Eq. (16) reveals that ion-exchange occurs preferentially in acidic and neutral solutions but diminishes quickly with increase of pH. Indeed it is normally considered that for pH < 9–10 ion exchange dominates glass corrosion whereas hydrolysis reactions are significant when pH exceeds 9 [12]. Note that Eq. (6) reveals that the hydrolytic rate holds exactly an opposite pH dependence $r_h \propto 10^{0.5\text{pH}}$ and the higher the pH the higher the hydrolytic rate. Thus glass corrosion occurs at low pH preferentially via diffusion-controlled ion exchange whereas at high pH via hydrolysis. Because of the opposite pH dependences of the two basic corrosion mechanisms the activation energies revealed in corrosion experiments are low (e.g. $E_{di}/2$) at low pH, and high (E_a) at high pH. For example, Grambow found acti- vation energies of corrosion $E_{cor} = 30$ kJ/mol at pH = 2.5–3.0 and $E_{cor} = 72$–77 kJ/mol at pH = 8.5–9.5 [35]. Expression (16) reveals that the rates of ion exchange depend on what type of ion is involved in, e.g. the rates are ionic selective. The rates of ion exchange with time diminish as the inverse square root of time reflecting the fact that near surface layers of glasses are depleted in cationic species and deeper and deeper layers are supplying cations for ion exchange reaction (1). As the total rate of released species into the water is given by the sum $r_i = r_{xi} + r_h$ we conclude that generically the time dependence of corrosion rate has the form $r_i \propto \text{const} + \text{const}_i\, t^{-0.5}$. All of the above dependences are in excellent agreement with experiments for both conventional and nuclear waste glasses [8,36–38].

Eq. (16) indicates that the ion exchange rate is determined completely by the effective diffusion coefficient D_i which depends on the pH of the attacking solution and has an Arrhenius temperature dependence of activation energy E_{di}. It is important to note however that according to [11] for irradiated glasses the temperature dependence of ion exchange is described by a two exponential function, and it has two activation energies – one high ($H_{mH} + H_{fNBO}$) at high temperatures and another low (H_{mH}) at low temperatures.

2.3. Normalised leaching rates

The term leaching is normally used to denote ion exchange release of species from glasses [6]. The average normalised leaching rate (due to ion exchange processes) NRx_i (g/cm^2 d) is measured experimentally or it can be found theoretically by calculating the total normalised cation release (e.g. normalised mass loss NMx_i, g/cm^2) and dividing it by the leach test duration t(d). The cation releases are fully determined by ion exchange reactions either when water solutions are silica saturated or for initial corrosion of glasses at $t \leqslant \tau(T)$. The normalised ion exchange release rate (nrx_i, g/cm^2 d) is given by

$$nrx_i = \frac{rx_i}{f_i}. \tag{17}$$

Hence NMx_i and NRx_i are given by

$$NMx_i = \frac{1}{f_i}\int_0^t rx_i\,\mathrm{d}t, \quad NRx_i = \frac{1}{f_i t}\int_0^t rx_i\,\mathrm{d}t. \tag{18}$$

Substituting Eq. (16) into Eq. (18) gives

$$NMx_i = 2\rho\left(\frac{D_i t}{\pi}\right)^{1/2}, \quad NRx_i = 2\rho\left(\frac{D_i}{\pi t}\right)^{1/2}. \tag{19}$$

The last expressions are widely used to quantify experimental results e.g. in the IAEA leaching test ISO6961-1982 [39]. However, Eq. (19) does not account for the decay of radioactive species which is important for nuclear waste glasses. Radioactive decay causes an exponential decrease of radionuclide concentrations in nuclear waste glasses. The equations for NMx_i and NRx_i, accounting for the decay of radioactive species such as ^{134,137}Cs, are as follows [5,8,31]:

$$\begin{aligned} NMx_i &= \rho\left(\frac{D_i}{\lambda_i}\right)^{1/2}\operatorname{erf}\left(\sqrt{\lambda_i t}\right), \\ NRx_i &= \frac{\rho}{t}\left(\frac{D_i}{\lambda_i}\right)^{1/2}\operatorname{erf}\left(\sqrt{\lambda_i t}\right), \end{aligned} \tag{20}$$

where λ_i is the decay constant (1/y), t is the testing time and erf(z) is the error function $\operatorname{erf}(z) = \frac{2}{\sqrt{\pi}}\int_0^z \exp(-x^2)\,\mathrm{d}x$. For stable cations $\lambda_i \to 0$ and Eq. (20) reduces to Eq. (19). However, for long term tests or short lived radionuclides, when the test duration is either close to or even exceeds the half-life of the radionuclides, $T_{1/2} = \ln 2/\lambda_i$, so that Eq. (20) must be used to calculate D_i correctly. Eqs. (20) and (19) enable quantification of effective diffusion coefficients D_i for different species [40,41]. Data on effective diffusion coefficients or interdiffusion coefficients in typical glasses can be found in [42], Table 2 gives D_i for several silicate glasses tested in near-neutral waters.

Data from Table 2 can be used to calculate the total inventory of released species from a given glass in water.

2.4. Radionuclide release inventory

The mass inventory of the ith radionuclide released from a nuclear waste glass M_i (g) is given by multiplying the normalised mass loss by the surface area of the glass in contact with water S and mass fraction of the i-radionuclide in the glass:

Table 2
Effective diffusion coefficients in some silicates

Glass	Cation	Temperature (°C)	D_i (m^2/s)	References
USA SM539	B	90	4×10^{-21}	[43]
	Li		7×10^{-21}	
	Na		4×10^{-21}	
British Magnox-waste	Li	40	1.9×10^{-20}	[44]
	Na		4.4×10^{-20}	
Russian O3O-6	Na	22	2.8×10^{-21}	[40]
Russian K-26	Cs	4.5	5×10^{-21}	[8]
Russian Bs-10	Cs	11	1.8×10^{-20}	[27]
Quartz artefacts[a]	H	6.6–24	$\sim10^{-25}$	[2]
Silica glass	H	23	1.4×10^{-21}	[2,45]

[a] Although these data are for crystalline quartz, it has been demonstrated that the hydration process occurs according to Doremus' diffusion–reaction mechanism [2].

$M_i = NM_iSf_i$. Thus the released fraction of the radionuclide i, ϕ_i, from a nuclear waste glass is $\phi_i = M_i/M_0$, where M_0 is the initial radionuclide content in the glass, e.g. $M_0 = f_i\rho V$, where V is the waste glass volume. For nuclear waste glasses ϕ_i can be found from

$$\phi_i = \frac{Sf_iNM_i}{f_i\rho V} = \frac{S}{\rho V}NM_{s_i} + \frac{S}{V}\left(\frac{D_i}{\lambda_i}\right)^{1/2}\mathrm{erf}(\sqrt{\lambda_i t}) + \frac{S}{V}\frac{r_\mathrm{h}}{\lambda_i}[1-\exp(-\lambda_i t)], \tag{21}$$

where NM_{si} is a constant accounting for instantaneous surface dissolution of near surface glass layers and adsorbed radionuclides. The second term in Eq. (21) accounts for ion exchange and the third for hydrolysis. Eq. (21) demonstrates that because of radioactive decay the inventory of radionuclides leached from nuclear waste glasses with time tends asymptotically to certain maximal values

$$\phi_i(t\to\infty) \to \frac{S}{\rho V}NM_{s_i} + \frac{S}{V}\left(\frac{D_i}{\lambda_i}\right)^{1/2} + \frac{S}{V}\frac{r_\mathrm{h}}{\lambda_i}. \tag{22}$$

For radioactive ^{137}Cs leached from Russian K-26 borosilicate waste glass for which it was found earlier that $D_\mathrm{Cs} = 5\times10^{-21}$ m^2/s and $r_\mathrm{h} = 0.1$ μm/y [8] the fractional inventory of radioactive ^{137}Cs leached out of nuclear waste glass K-26 will not exceed the maximal value $\phi_\mathrm{Cs} = 2.75\times10^{-5}$. In contrast to this for stable species which hold $\lambda_i = 0$ from (21) it follows that $\phi \to 1$ when $t\to\infty$ demonstrating that the decay significantly diminishes the overall release of species into the environment.

2.5. Contribution of ion exchange

To determine the contribution of ion exchange to the overall release of radionuclides we can compare the second and the third terms in the equation of radionuclide releases (21) via ratio, F

$$F(t) = \frac{(\phi_i)_\text{Ion-exchange}}{(\phi_i)_\text{Hydrolysis}} = \left(\frac{D_i\lambda_i}{r_\mathrm{h}^2}\right)^{1/2}\frac{\mathrm{erf}(\sqrt{\lambda_i t})}{1-\exp(-\lambda_i t)}. \tag{23}$$

This equation shows that the contribution of ion exchange is initially dominant in all glasses although with time it diminishes and tends to a constant value. Such behaviour is demonstrated by Fig. 2, which shows the time dependence of parameter F for K-26 nuclear waste glass. Moreover from Eq. (23) it follows that the K-26 glass holds F(16y) = 2.03 which indicates about a 64% contribution of

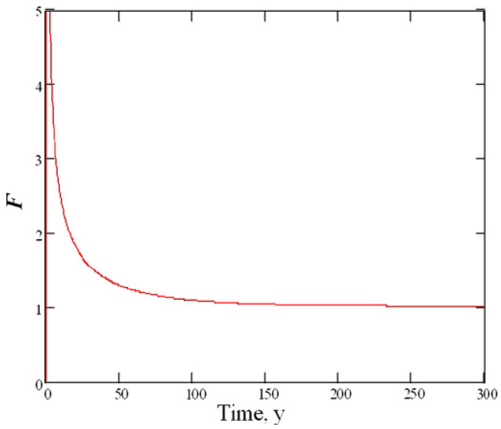

Fig. 2. Ratio of ion exchange to hydrolysis contributions in the overall release of ^{137}Cs from radioactive waste glass K-26.

ion exchange to the overall release of radionuclides. This result is in good agreement with calculations using the STORM computer code which predicted ~60% contribution from ion exchange [46]. Fig. 2 shows that the parameter F will further diminish with time but its value will remain higher than unity, which means that the ion exchange contribution to corrosion will remain higher than 50%, which is also consistent with the results of [46].

Both Eq. (23) and Fig. 3 show that for very long times significantly exceeding the radionuclide half-lives, $t \gg T_{1/2}$, the parameter F tends to a constant value

$$F(t \to \infty) \to \frac{(D_i \lambda_i)^{1/2}}{r_{\mathrm{h}}}. \tag{24}$$

The higher the diffusion coefficient the higher the contribution from ion exchange in the overall release of radionuclides from glasses. However in conditions when the hydrolysis is suppressed, such as in silica-saturated water solutions, and the hydrolysis rate is very small $r_{\mathrm{h}} \to 0$ the ion exchange contribution is overwhelming and $F \to \infty$. Under such conditions hydrolysis can simply be ignored in the analysis of radionuclide release. In addition, from Eq. (24) it follows that for short-lived radionuclides which hold higher decay constants, λ_i, the role of ion exchange is more significant than for long-lived radionuclides.

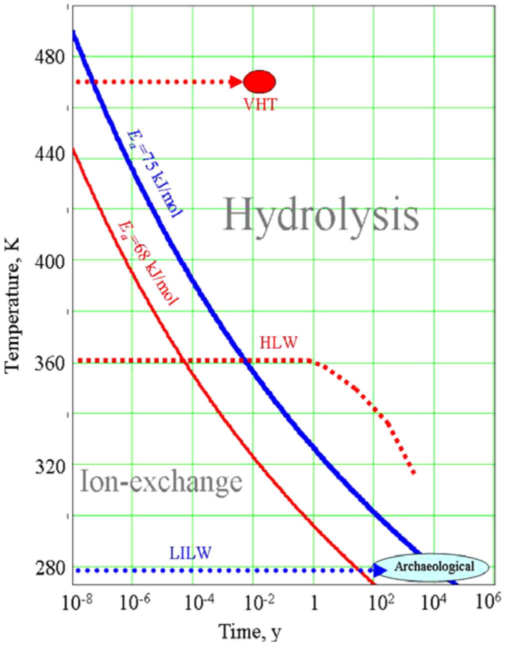

Fig. 3. Time–temperature characterisation of corrosion mechanisms of silicate glasses.

2.6. Universal time–temperature behaviour

The characteristic time $\tau(T)$ given by Eq. (7) can be used to describe the time–temperature corrosion behaviour of nuclear waste glasses. The glasses corrode in non-silica-saturated solutions via diffusion-controlled ion exchange up to time $\tau(T)$. The hydrolytic stage of glass corrosion is dominant when time $t \geqslant 16\tau(T)$, whereas within $\tau(T) \leqslant t \leqslant 16\tau(T)$ the glass corrodes with equivalent contributions from both ion exchange and hydrolysis. The activation energies of the hydrolyses are typically much higher than those of diffusion-controlled processes, and it is known that over a wide variety of glass compositions E_{a} is in the range 70–90 kJ/mol [47]. Because $2E_{\mathrm{a}} \gg E_{\mathrm{di}}$ the term E_{di} can be dropped from (7) giving a universal equation, which separates the ion exchange from hydrolysis contributions in time–temperature $\{t, T\}$ coordinates

$$\ln\left(\frac{\tau(T)}{\tau_0}\right) = \frac{2E_{\mathrm{a}}}{RT}. \tag{25}$$

Fig. 3 shows the corrosion behaviour of typical nuclear waste borosilicate glasses in non-saturated conditions in $\{t, T\}$ coordinates for two glasses with $E_{\mathrm{a}} = 68$ and 75 kJ/mol.

Fig. 3 can be used to give insight into the mechanisms of glass corrosion for various conditions of corrosion processes or tests. For example, the vapour hydration test (VHT) is currently used as an accelerated corrosion test [48]. Conditions envisaged in this test are situated on the $\{t, T\}$ map in the hydrolytic area mainly due to the high temperatures applied. In contrast to VHT archaeological glasses would be located in the hydrolytic area due to the long times of alteration rather than because of high temperatures. However, some intermediate age glasses such as those corroding in sea water [2] can still undergo the phase of ion-exchange. Note also ninth century soda-lime-silica glasses, which are in a relatively dry soil environment, exhibit corrosion by ion exchange leaching, rather than by dissolution [49]. It is expedient therefore to compare similar composition archaeological glasses from colder places, which hold an extended period of diffusion-controlled ion exchange, with glasses from warmer sites, which have already passed to a hydrolytic regime of corrosion. HLW glasses in non-silica saturated conditions at high temperatures pass quickly to a hydrolytic corrosion regime, however when cooled to environmental temperatures these will (like LILW glasses), corrode for many tens to hundreds of years via ion exchange. For example at the minimum value of dissolution rate 0.002 μ/y for R7T7 glasses R7T7 [50] the ion exchange period will last for >1500 years. In silica saturated conditions $\tau 0 \to \infty$ and the ion exchange stage will persist for geological timescales. Note that silica saturated conditions can also occur due to corrosion of the glass itself if the volume of contacting water is small [51]. This situation is not analysed here as we supposed that the contacted water is diluted and kept at constant parameters. In this case, because it changes with time r_h and consequently $\tau(T)$, the ion exchange phase will control both the initial and final stages of glass corrosion; the intermediate phase being controlled by hydrolysis.

2.7. Experiment on magnox waste glass

To investigate applicability of some above-discussed parameters a series of leaching tests were performed on simulated magnox waste (MW) glass at temperatures 40, 50 and 60 °C for 27 days each. Glass fibers of about 0.5 mm in diameter and 50 mm length were used in the tests. This form of specimen was chosen to avoid mechanical reprocessing (cutting, grinding, and polishing) that could result in changing properties of glass surface. Composition of the glass samples used is given in Table 3. This composition was simplified compared to the published data on simulant glass studies.

Batch dissolution experiments were conducted at 40, 50 and 60 °C using an original methodology combining traditional static leaching methods with the pass-flow tests. Experiments were conducted for periods up to 27 days with intermediate probe-sampling and solution refreshment after 3, and 15 days since the beginning of test. At each probe sampling pH of aliquots were measured. Though leaching tests were carried out in distilled water and no pH adjustment was done, pH shift during the leaching was quite small. After 3 days leaching pH of solution was 6.1 (pH of fresh distilled water used is 6.0). And to the end of experiments it shifted to 6.2–6.3.

Table 3
Chemical compositions of simulated MW glass (calculated from the batch mix), wt%

Al_2O_3	4.90	La_2O_3	3.61	P_2O_5	0.20
B_2O_3	17.17	Li_2O	3.82	SiO_2	47.94
BaO	0.62	MgO	5.37	SrO	0.32
Cs_2O	1.03	MoO_3	1.62	Y_2O_3	0.19
Fe_2O_3	3.13	Na_2O	8.51	ZrO_2	1.57

PTFE containers of 100 ml capacity were used for leaching tests. Volume of water used in each single run was 90 ml. Surface area to solution volume ratio was in range 3–4 m^{-1}. Containers used were of the size that glass fibers put in the container couldn't lay flat on the bottom. No additional specimen support was necessary and almost all surface of the specimen was in contact with water. Cleaning of new and used containers has been done according to the procedure described in MCC-1 leaching test procedure. Concentrations of Na, Li, Mg, B, Si, and Mo in aliquots were measured using ICP-MS.

Normalised Elemental Mass Loss (NL), $g\,m^{-2}$, was calculated from

$$NL = \frac{m_i}{f_i \cdot S}, \tag{26}$$

where m_i is total leached mass of the component i (g), f_i is the fraction of element i in glass (dimensionless), and S is the surface area of the glass sample (m^2). The value of m_i was obtained as sum of ith element mass losses at all steps of test and it was calculated as the ΔC – difference in concentration of element i at the beginning and the end of step multiplied by V – the volume of leaching solution

$$m_i = \sum_n \Delta C_n \cdot V_n, \tag{27}$$

where n denotes the number of leaching step. The volume V remains 90 ml during the whole test. ΔC at each step is found as

$$\Delta C = C_{i1} - C_{i0}, \tag{28}$$

where C_{i1} is the concentration of element i measured in the probes taken from the solution in the end of each step. C_{i0} is calculated from the measured concentration in the end of the previous step of test as

$$(C_{i0})_n = (C_{i1})_{n-1} \cdot \frac{V_n - \Delta V}{V_n}, \tag{29}$$

where $(C_{i1})_{n-1}$ is the concentration of element i measured in aliquot taken in previous step, ΔV is the volume of solution refreshed, including volume of aliquot, and V_n is the volume of solution at the current step which is constant.

Normalised leach rate NR_i ($g\,m^{-2}\,d^{-1}$) were calculated from

$$NR_i = \frac{NL_i}{t}, \tag{30}$$

where t is duration of sample leaching (days).

Effective diffusion coefficient D, $m^2\ s^{-1}$ calculated from the leaching rate of alkaline elements assuming that it occurs via ion-exchange as [39–41]

$$D = \frac{NR^2 \pi t}{4\rho^2}, \tag{31}$$

that follows from the Eq. (19).

Generally, uncertainty estimates for the calculated rates were determined by standard error propagation methods, assuming uncorrelated random errors. In this case, the standard deviation of a function $f(x_1, x_2, \ldots, x_n)$ is given by

$$\sigma_f = \sqrt{\sum_{i=1}^{n} \left(\frac{\partial f}{\partial x_i}\right)^2 \sigma_i^2}, \tag{32}$$

where σ_f is the standard deviation of the function f, x_i the parameter i, σ_i is the standard deviation of parameter i. Assuming following measurements' errors in the error calculation the resulting errors of NL, NR and D calculated are in the range of 12–15%.

MW glass shows a typical dissolution plot (Fig. 4). At the beginning of the test the leaching rate has the maximum value due to sharp concentration gradient between glass and water. With time, as the leaching proceed this gradient become smoother, and the leaching rate decreases.

MW glass dissolution is an incongruent process. Na has the highest release rate (Table 4), whereas network-forming elements such as Si and Mo show lower release rates. Data published display that dissolution rate of B from borosilicate glasses is usually much higher than that of Si despite the fact that both elements are major network former [32]. This probably occurs because of their different position in the glass structure as Si forms [SiO_4] tetrahedra while B at least partly is hold in [BO_3] triangles, as well as high mobility of B in aqueous media.

Table 4
Normalised release rates and activation energies of elemental release from MW glass measured at 27 days leaching test, 10^{-2} g/m^2day

	40 °C	50 °C	60 °C
Na	3.36	5.72	7.53
Li	2.20	4.74	7.05
Mg	2.36	4.74	6.96
B	2.46	5.56	8.22
Si	1.76	4.42	5.02
Mo	1.43	3.91	4.41

Fig. 5(a) shows a plot of the logarithm of release rates for main elements MW glass versus reciprocal of the absolute temperature. The rate values are normalised release rates calculated on 27 days leaching. The apparent activation energy of release (E_{act}, $J\ mol^{-1}$) may be calculated from the data obtained. According to the Arrhenius equation the gradient of these plots has the value $-E_{act}/R$, where R is the gas constant ($8.314\ J\ K^{-1}\ mol^{-1}$). Activation energy was calculated for three leaching duration times.

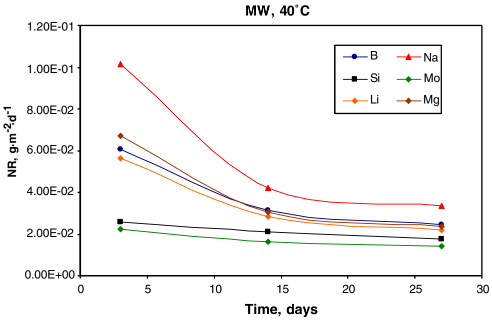

Fig. 4. Normalised release rate plot vs. time showing leaching of main MW constituents from the glass at 40 °C.

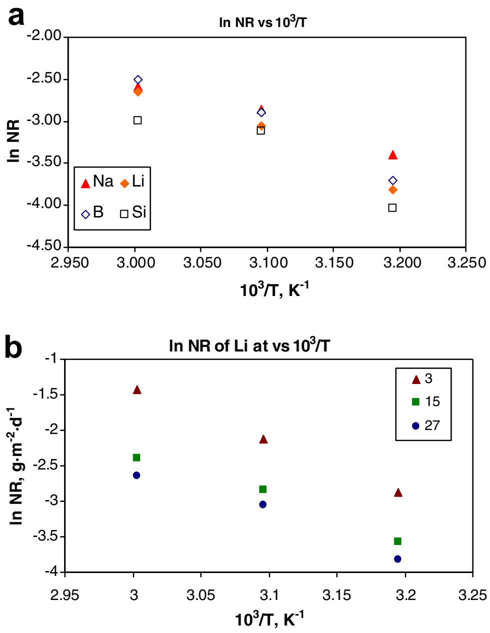

Fig. 5. Normalised elemental release rates calculated from 27 days leaching of MW glass vs reciprocal temperature (a) and normalised release rates calculated from 3, 15 and 27 days leaching of Li from MW glass vs. reciprocal temperature (b).

Table 5
Apparent activation energy of elemental release, kJ/mol

Leaching duration	3 days[a]	27 days[a]	18 h[b]	18 h[b]
pH	6.1	6.2	2.3	12.1
Na	39.1	35.1		
Li	62.9	50.6	18	62
Mg	50.9	47.0		
B	63.3	52.5	18	64
Si	86.4	45.7	32	56
Mo	80.0	49.3		

[a] Results of current work.
[b] Data from [32].

Table 6
Diffusion coefficients of alkalis in simulated MW glass, m^2/s

	Duration, days	Temperature (°C)		
		40	50	60
Na	3	4.4×10^{-20}	7.6×10^{-20}	2.7×10^{-19}
Li	3	1.4×10^{-20}	6.1×10^{-20}	2.5×10^{-19}
Na	27	4.4×10^{-20}	1.3×10^{-19}	2.2×10^{-19}
Li	27	1.9×10^{-20}	8.7×10^{-20}	1.9×10^{-19}

Similar gradients of Li *NR* plots suggest close E_{act} values for the rate of Li release from MW glass after 3, 15 and 27 days of leaching (Fig. 5(b)). The same is true for most of MW constituents. The plot reveals that the data corresponded to short-term leaching (3 days) fit Arrhenius dependence better that those of 15 and 27 days leaching.

Apparent activation energies of elemental release are shown in Table 5 along with data reported for MW glass dissolution at pH 2.3 and 12.1 [32].

Effective diffusion coefficients of alkaline elements in MW glass are presented in Table 6.

There are few data published on effective diffusion coefficient measured by leaching of alkalis, and direct comparison of our data with the published ones is difficult because of differences in glass composition or in experiment conditions (Table 2). For instance, the effective diffusion coefficients measured on a series of Na-borosilicate glasses from one day leaching in deionised water at 22 °C are in good agreement with those obtained in our study. The values reported are in the range $(4\text{–}5) \times 10^{-19}$ m^2/s (compositions Nos. 4 and 5 in [40]).

3. Conclusions

Diffusion-controlled ion exchange governs the initial stages of glass corrosion in water solutions and remains important until times $t = 16\tau(T)$ in non-saturated solutions, and persists at geological timescales in silica-saturated conditions. The ion exchange corrosion rate diminishes as the square root of time because of gradual depletion of cations from glass near-surface layers. The temperature dependence of corrosion rate follows Arrhenius kinetics with a universal activation energy for most monovalent cations. The ion exchange rate decreases as $10^{-0.5\text{pH}}$ with increased pH of the contacting water. Ion exchange contributes significantly to the overall inventory of radionuclide release from nuclear waste glasses, being most important for short-lived radionuclides.

Acknowledgements

Authors are grateful to Professors V. Stolyarova and B. Grambow for useful discussions and Drs D. Strachan, B. Burakov and O. Batyukhnova for important suggestions.

References

[1] A. Silvestri, G. Molin, G. Salviulo, J. Non-Cryst. Solids 351 (2005) 1338.
[2] J.E. Ericson, O. Dersch, F. Rauch, J. Archaeol. Sci. 31 (2004) 883.
[3] M.I. Ojovan, W.E. Lee, An Introduction to Nuclear Waste Immobilisation, Elsevier Science Publishers B.V., Amsterdam, 2005.
[4] M.I. Ojovan, A.S. Pankov, W.E. Lee, R.J. Hand, in: Proceedings of the WM'05 Conference, Tucson, Arizona, 2005, 11p., 5114.pdf.
[5] M.I. Ojovan, W.E. Lee, R.J. Hand, in: Proceedings of the ICEM'05, ICEM05-1170, ASME, 2005.
[6] A.A. Appen, Chemistry of Glass, Khimiya, Leningrad, 1970, p. 352.
[7] A.A. Belyustin, M.M. Shultz, Glass Phys. Chem. 9 (1983) 3.
[8] M.I. Ojovan, R.J. Hand, N.V. Ojovan, W.E. Lee, J. Nucl. Mater. 340 (2005) 12.
[9] Engineered barrier systems and the safety of deep geological repositories. Report EUR 19964 EN, OECD, Issy-Ies-Moulineaux, 2003.
[10] T. Advocat, P. Jollivet, J.L. Crovisier, M. del Nero, J. Nucl. Mater. 298 (2001) 55.
[11] M.I. Ojovan, W.E. Lee, J. Nucl. Mater. 335 (2004) 425.
[12] W.E. Lee, M.I. Ojovan, M.C. Stennett, N.C. Hyatt, Adv. Appl. Ceramics 105 (1) (2006) 3.
[13] S.V. Stefanovsky, S.V. Yudintsev, R. Giere, G.R. Lumpkin, in: Energy Waste and the Environment: a Geochemical Perspective, vol. 236, Geological Society, Special Publications, London, 2004, p. 36.
[14] I.L. Pegg, I. Joseph, in: C. Ho Oh (Ed.), Hazardous and Radioactive Waste Treatment Technologies Handbook, CRC, Boca Raton, 2001, p. 4.2.1.
[15] M. Denton, C. Nigl, K. Wiemers, Proceedings of the ICEM'05, ICEM05-1470, ASME, 2005.

[16] M.-J. Song, Nucl. Eng. Int. (February) (2003) 22.

[17] C.A. Calle, A. Luce, Proceedings of the ICEM'01, ASME, 2001, 259pdf.

[18] I.A. Sobolev, S.A. Dmitriev, F.A. Lifanov, A.P. Kobelev, S.V. Stefanovsky, M.I. Ojovan, Glass Technol. 46 (2005) 28.

[19] Scientific and technical basis for near-surface disposal of low and intermediate level waste. TRS-412, IAEA, Vienna, 2003.

[20] R.H. Doremus, J. Non-Cryst. Solids 48 (1982) 431.

[21] P. Agaard, H.C. Helgeson, Am. J. Sci. 282 (1982) 237.

[22] B.P. McGrail, A. Kumar, D.E. Day, J. Am. Ceram. Soc. 67 (1984) 463.

[23] T.V. Antropova, J. Non-Cryst. Solids 345&346 (2004) 270.

[24] D.H. Bacon, B.P. McGrail, Mater. Res. Soc. Symp. Proc. 757 (2003) II1.9.1.

[25] W.L. Ebert, Phys. Chem. Glasses 34 (1993) 58.

[26] B.P. McGrail, W.L. Ebert, A.J. Bakel, D.K. Peeler, J. Nucl. Mater. 249 (1997) 175.

[27] M.I. Ojovan, W.E. Lee, R.J. Hand, N.V. Ojovan, Proceedings of the XX International Congress on Glass, Kyoto, Japan, 2004, sr00700033DIS.pdf.

[28] M.I. Ojovan, W.E. Lee, A.S. Barinov, N.V. Ojovan, I.V. Startceva, D.H. Bacon, B.P. McGrail, J.D. Vienna, Mater. Res. Soc. Symp. Proc. 824 (2004) CC5.8.1.

[29] W.A. Weyl, J. Non-Cryst. Solids 19 (1975) 1.

[30] M. Ojovan, G. Moebus, N. Ojovan, C. McLeod, A. Cox, ICP Inform. Newslett. 30 (2005) 1022.

[31] S.A. Dmitriev, A.S. Barinov, N.V. Ozhovan, I.V. Startseva, Z.I. Golubeva, I.A. Sobolev, M.I. Ozhovan, Atomic Energy 98 (2005) 196.

[32] P.K. Abraitis, F.R. Livens, J.E. Monteith, J.S. Small, D.P. Triverdi, D.J. Vaughan, R.A. Wogelius, Appl. Geochem. 15 (2000) 1399.

[33] B.M.J. Smets, M.G.W. Tholen, Phys. Chem. Glasses 26 (1985) 60.

[34] J.R. Manning, in: Diffusion. Papers Presented at a Seminar of the American Society for Metals, October 14 and 15, 1972, American Society for Metals, Metal Park, OH, 1973, p. 1.

[35] B. Grambow, Glastech. Ber. 56 (1983) 566.

[36] M.A. Rana, R.W. Douglas, Phys. Chem. Glasses 2 (1961) 179.

[37] Chemical durability and related properties of solidified high-level waste forms, TRS-257, IAEA, Vienna, 1985.

[38] S. Portal, R. Sempere, Phys. Chem. Glasses 44 (2003) 303.

[39] E. Hespe, Atomic Energy Rev. 9 (1977) 145.

[40] I.A. Ivanov, S.V. Stefanovsky, A.N. Gulin, Glass Phys. Chem. 19 (1993) 746.

[41] I. Plecas, R. Pavlovich, S. Pavlovic, J. Nucl. Mater. 270 (2004) 171.

[42] R.H. Doremus, in: Diffusion. Papers presented at a Seminar of the American Society for Metals, October 14 and 15, 1972, American Society for Metals, Metal Park, Ohio, 1973, p. 333.

[43] M. Aertsens, K. Lemmens, P. Van Iseghem, Mater. Res. Soc. Symp. Proc. 757 (2003) II5.8.1.

[44] A. Pankov, M.I. Ojovan, W.E. Lee, C.R. Scales, in: Proc ICEM'05, ASME, 2005, ICEM05-1130.

[45] A. Zoune-Thimm, Doctoral dissertation, J.W. Goethe-Universitat. Frankfurt Main, 1999.

[46] D.H. Bacon, M.I. Ojovan, B.P. McGrail, N.V. Ojovan, I.V. Startceva, in: Proceedings of the ICEM '03, ASME, Oxford, England, 2003, 4509.pdf.

[47] D.M. Strachan, J. Nucl. Mater. 298 (2001) 69.

[48] A. Jiricka, J.D. Vienna, P. Hrma, D.M. Strachan, J. Non-Cryst. Solids 292 (2001) 25.

[49] C.P. Stapleton, S.E. Swanson, Mater. Res. Soc. Symp. Proc. 757 (2003) II2.5.1.

[50] D. Mallants, J. Marivoet, X. Sillen, Performance assessment of the disposal of vitrified high-level waste in a clay layer, J. Nucl. Mater. 298 (2001) 125.

[51] I.A. Sobolev, M.I. Ojovan, T.D. Scherbatova, O. G Batyukhnova, Glasses for radioactive waste, Energoatomizdat, Moscow, 1999, p. 238.